Inorganica Chimica Acta 363 (2010) 1114–1125

Contents lists available at ScienceDirect

Inorganica Chimica Acta

journal homepage: www.elsevier.com/locate/ica

Group 3 complexes incorporating (furyl)-substituted disilazide ligands

Lloyd T.J. Evans, Martyn P. Coles *, F. Geoffrey N. Cloke *, Peter B. Hitchcock

Department of Chemistry, University of Sussex, Falmer, Brighton BN1 9QJ, UK

ARTICLE INFO

Article history:
Received 17 July 2009
Received in revised form 15 September 2009
Accepted 27 September 2009
Available online 6 October 2009

Dedicated to Professor Jon Dilworth, with sincere thanks for all his support and encouragement over the years.

Keywords:
Amide
Scandium
Yttrium
Aryloxide
Organolanthanide

ABSTRACT

A series of *mono*- and *bis*-amide scandium and yttrium compounds incorporating the furyl-substituted disilazide ligand, $[N\{SiMe_2R\}_2]^-$ {**i**} (where R = 2-methylfuryl) have been synthesized. The compounds $Sc\{\mathbf{i}\}Cl_2$ (**1**), $Sc\{\mathbf{i}\}(CH_2SiMe_3)_2$ (**2**) and $Sc\{\mathbf{i}\}(OAr)_2$ (**3**) were made from suitable scandium starting materials employing either a salt metathesis protocol with Li{**i**} or *via* protonolysis of Sc–C bonds by the neutral amine H{**i**}. The thermally unstable *bis*-alkyl yttrium compound, '$Y\{\mathbf{i}\}(CH_2SiMe_3)_2$' was isolated as the *bis*-THF adduct (**4**) and the *bis*-aryloxide $Y\{\mathbf{i}\}(OAr)_2$ (**5**) was synthesized by elimination of LiOAr from $Y(OAr)_3$. The *bis*-amide complex $Y\{\mathbf{i}\}_2Cl$ (**6**) and conversion to a rare example of an yttrium benzyl compound $Y\{\mathbf{i}\}_2(CH_2Ph)$ (**7**) are described. The yttrium cation, $[Y\{\mathbf{i}\}_2]^+$, was synthesized by benzyl abstraction from **7** using $B(C_6F_5)_3$. Structural characterization of representative examples show variation in the coordination modes for amide ligand {**i**}, differing primarily in the number of furyl groups that coordinate to the metal, with examples in which zero, one or two $M–O_{furyl}$ bonds are present. Preliminary investigation in two areas of catalysis are presented.

1. Introduction

Compounds of group 3 metals, in particular the lighter members of the group scandium and yttrium, continue to be developed as catalysts in a number of important chemical transformations including olefin polymerization [1–7] and hydroamination [8,9]. Key to the success of these compounds is the presence of an ancillary ligand set that will regulate the balance between supporting the active component of a catalytic system whilst preventing decomposition through side-reactions. As with the transition elements, the cyclopentadienyl anion, and derivatives thereof, have played a central role in the chemistry of these elements. However, the search for alternatives to these organometallic ligands represents an important area of chemical research, with the potential to open up this area of chemistry to wider applications.

Although simple amides, $[NR_2]^-$, represent an important class of ligand in coordination chemistry [10], the incorporation of additional functionalities that are able to interact with metal centres frequently offers considerable advantage in catalytic applications, where lability of one or more components enables substrates to approach the metal whilst being able to offer stabilization to active species formed during the catalysis. We have recently investigated a class of silyl-substituted amide ligands incorporating furyl-substituents at silicon [11–13], and have reported a range of main group (Li, K, Mg, Al) and transition-metal (Ti, Zr) compounds incorporating this class of ligand. It was found that the 2-methylfuryl derivative, $[N\{SiMe_2R\}_2]^-$ ($R = 2\text{-}MeC_4H_2O$) generally gave the most favourable combination of solubility and stability to complexes, and this paper describes the application of this ligand, (the neutral form of the ligand is abbreviated to H{**i**} in this manuscript) in the chemistry of the group 3 elements, scandium and yttrium.

During previous crystallographic studies we have identified several bonding modes for ligand {**i**} that differ in the number of furyl groups that bond to the metal (Fig. 1). For example, the aluminium complex $Al\{\mathbf{i}\}Cl_2(THF)$ contained an κ*N*-bound {**i**} ligand, which we abbreviate as an **A**-type bonding [13]. When the THF was removed by sublimation of the product, this binding mode was converted to a tridentate κ*N*,*O*,*O*′- or **C**-type bonding in $Al\{\mathbf{i}\}Cl_2$ [13]. In contrast, the dimeric zirconium compound $[Zr\{\mathbf{i}\}Cl_3]_2$ had octahedral metals in which the amide was bound with a heteroditopic κ*N*,*O*- or **B**-type coordination [12]. It is important to note, however, that these coordination modes are describing the solid-state structures and that the situation in solution may be fluxional. This is best illustrated in compounds in which the **B**-type coordination is present in the solid-state, where routinely only one set of furyl resonances is observed by NMR spectroscopy.

* Corresponding authors. Fax: +44 (0)1273 677196 (F.G.N. Cloke).
E-mail addresses: m.p.coles@sussex.ac.uk (M.P. Coles), f.g.cloke@sussex.ac.uk (F.G.N. Cloke).

0020-1693/$ - see front matter © 2009 Elsevier B.V. All rights reserved.
doi:10.1016/j.ica.2009.09.051

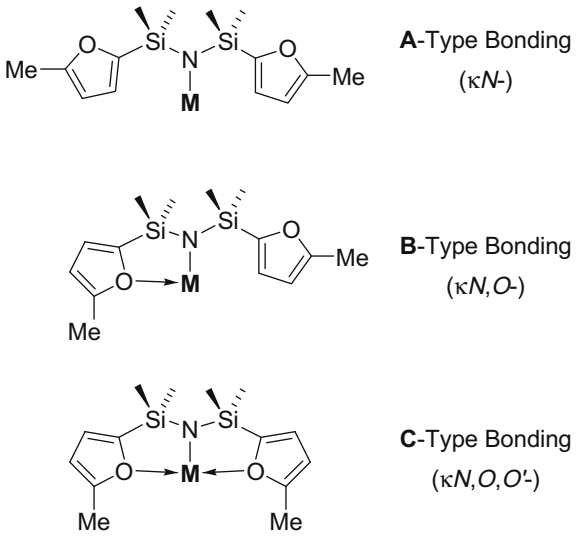

Fig. 1. Previously observed bonding modes for ligand {**i**} at a single metal centre.

2. Experimental

2.1. General considerations

All manipulations were carried out under dry argon using standard Schlenk-line and cannula techniques, or in a conventional nitrogen-filled glovebox. Solvents were dried over appropriate drying agent and degassed prior to use. NMR spectra were recorded using a Bruker Avance DPX 300 MHz spectrometer at 300.1 (^{1}H) and 75.4 (^{13}C{^{1}H}) MHz, from samples at 25 °C in [$^2H_6$]-benzene, unless otherwise stated. Coupling constants are quoted in Hz, and assignments are according to Fig. 2. Proton and carbon chemical shifts were referenced internally to residual solvent resonances. Elemental analyses were performed by S. Boyer at London Metropolitan University; GPC Analyses were carried out by Smithers Rapra Technology.

HOAr (Ar = 2,6-^{t}Bu$_2$C$_6$H$_3$) was sublimed prior to use. $YCl_3(THF)_3$ was prepared by refluxing anhydrous YCl_3 in excess tetrahydrofuran for 24 h at 75 °C, followed by removal of volatiles under reduced pressure. $ScCl_3(THF)_3$ [14], KCH_2Ph [15], $Sc(CH_2SiMe_3)_3(THF)_2$ [16], and $Y(CH_2SiMe_3)_3(THF)_2$ [17] (these reagents were also generated from the reaction of the metal trichloride with $LiCH_2SiMe_3$ [18] in THF, and were used without isolation) $Sc(OAr)_3$, $Y(OAr)_3$ [19], and Li{**i**} [{**i**} = N{SiMe$_2$R}$_2$ (where R = 2-methylfuryl)] [11] were made according to previously published procedures.

2.2. Synthesis of Sc{*i*}Cl$_2$ (*1*)

THF (60 mL) was added to a dry mixture of anhydrous $ScCl_3$ (500 mg, 3.3 mmol) and Li{**i**} (987 mg, 3.3 mmol) and the resulting suspension heated to 70 °C with stirring for 5 days. All volatiles were then removed *in vacuo* and the residue extracted with toluene (60 mL). The extract was filtered through celite to remove LiCl. The resulting clear, colourless solution was concentrated *in vacuo* to approximately 10 mL and cooled to −45 °C, to afford the product as a colourless crystalline solid. Isolated yield = 810 mg, 60%. The more soluble precursor $ScCl_3(THF)_3$ can also be used in this preparation. *Anal.* Calc. for $C_{14}H_{22}NCl_2O_2ScSi_2$ (408.36): C, 41.18; H, 5.43; N, 3.43. Found: C, 41.26; H, 5.29; N, 3.56%. **^{1}H NMR**: δ 6.44 (d, *J* = 3.0, 2H, furyl-C*H*$_\alpha$) 5.82 (m, *J* = 3.0, 2H, furyl-C*H*$_\beta$) 2.38 (s, 6H, furyl-C*H*$_3$) 0.50 (s, 12H, Si*Me*$_2$). **^{13}C NMR**: δ 161.0 (furyl-*C*4) 156.5 (furyl-*C*3) 121.2 (furyl-*C*2) 107.6 (furyl-*C*1) 14.1 (furyl-*C*H$_3$) 3.6 (Si*Me*$_2$).

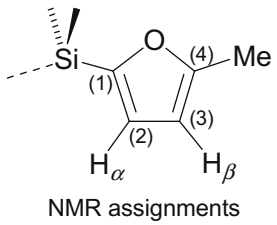

Fig. 2. NMR assignments used in this manuscript.

2.3. Synthesis of Sc{*i*}(CH$_2$SiMe$_3$)$_2$ (*2*)

Method 1: A solution of $LiCH_2SiMe_3$ (384 mg, 4.08 mmol) in pentane (30 mL) was added drop wise to a rapidly stirred slurry of $ScCl_3(THF)_3$ (500 mg, 1.36 mmol) in pentane (40 mL) at −78 °C. The resulting colourless suspension was allowed to warm up to ambient temperature, and a solution of H{**i**} (11.2 mL of a 0.122 M solution in pentane, 1.36 mmol) was added. After a further 30 min stirring, the resulting slightly yellow suspension was filtered through celite, giving a clear yellow solution. This was concentrated *in vacuo* to approximately 10 mL and cooled to −45 °C to afford the product as large yellow crystals. Isolated yield = 350 mg, 50%.

Method 2: Pre-chilled pentane (60 mL) was added to a dry mixture of $ScCl_3(THF)_3$ (500 mg, 1.36 mmol) $LiCH_2SiMe_3$ (256 mg, 2.72 mmol) and Li{**i**} (407 mg, 1.36 mmol) at −78 °C. The resulting suspension was allowed to warm up slowly to ambient temperature overnight. The solution was filtered through celite, giving a clear yellow solution. This was concentrated *in vacuo* to approximately 10 mL and cooled to −45 °C to afford the product as large yellow crystals. Isolated yield = 350 mg, 50%. *Anal.* Calc. for $C_{22}H_{44}NO_2ScSi_4$ (511.89): C, 51.62; H, 8.66; N, 2.74. Found: C, 51.79; H, 8.55; N, 2.85%. **^{1}H NMR**: δ 6.33 (d, *J* = 3.0, 2H, furyl-C*H*$_\alpha$) 5.75 (m, *J* = 3.0, 2H, furyl-C*H*$_\beta$) 2.48 (s, 6H, furyl-C*H*$_3$) 0.38 (s, 12H, Si*Me*$_2$) 0.09 (s, 4H, C*H*$_2$SiMe$_3$) 0.02 (s, 18H, CH$_2$Si*Me*$_3$). **^{13}C NMR**: δ 163.8 (furyl-*C*4) 156.8 (furyl-*C*3) 120.4 (furyl-*C*2) 109.0 (furyl-*C*1) 40.8 (*C*H$_2$SiMe$_3$) 15.3 (furyl-*C*H$_3$) 4.9 (CH$_2$Si*Me*$_3$) 3.3 (Si*Me*$_2$). **Mass spec.** (EI, *m*/*z*): 496 [M−CH$_3$]$^+$, 424 (M−CH$_2$SiMe$_3$]$^+$, 336 [Sc{**i**}]$^+$.

2.4. Synthesis of Sc{*i*}(OAr)$_2$ (Ar = 2,6-^{t}Bu$_2$C$_6$H$_3$, *3*)

Hexane (30 mL) was added to a dry mixture of Sc{**i**}(CH$_2$SiMe$_3$)$_2$ (200 mg, 0.39 mmol) and 2,6-di-*tert*-butylphenol (161 mg, 0.78 mmol) and the resulting solution stirred at ambient temperature for 1 h. The solution was then concentrated *in vacuo* to approximately 5 mL, and cooled slowly to −45 °C to afford the product as small white crystals. Isolated yield = 140 mg, 48%. *Anal.* Calc. for $C_{42}H_{64}NO_4ScSi_2$ (748.09): C 67.43; H, 8.62; N, 1.87. Found: C, 67.39; H, 8.69; N, 1.98%. **^{1}H NMR**: δ 7.26 (d, *J* = 6.0, 4H, *m*-C*H*) 6.82 (t, *J* = 7.5, 2H, *p*-C*H*) 6.33 (d, *J* = 3.0, 2H, furyl-C*H*$_\alpha$) 5.66 (m, *J* = 3.0, 2H, furyl-C*H*$_\beta$) 2.03 (s, 6H, furyl-C*H*$_3$) 1.46 (s, 36H, C*Me*$_3$) 0.45 (s, 12H, Si*Me*$_2$). **^{13}C NMR**: δ 163.0 (furyl-*C*4) 162.2 (*i*-*C*$_6$H$_3$) 157.6 (furyl-*C*3) 138.4 (*o*-*C*$_6$H$_3$) 126.0 (*m*-*C*$_6$H$_3$) 121.2 (furyl-*C*2) 118.8 (*p*-*C*$_6$H$_3$) 108.3 (furyl-*C*1) 35.5 (*C*Me$_3$) 32.7 (*CMe*$_3$) 14.5 (furyl-*C*H$_3$) 4.8 (Si*Me*$_2$). **Mass spec.** (EI, *m*/*z*): 541 [M−OAr]$^+$, 336 [Sc{**i**}]$^+$.

2.5. Synthesis of Y{*i*}(CH$_2$SiMe$_3$)$_2$(THF)$_2$ (*4*)

A solution of $LiCH_2SiMe_3$ (343 mg, 3.65 mmol) in pentane (30 mL) was added drop wise to a rapidly stirred slurry of $YCl_3(THF)_3$ (500 mg, 1.22 mmol) in pentane (40 mL) at −78 °C. The resulting colourless suspension was allowed to warm up to

ambient temperature, and a solution of H{**i**} (10 mL of a 0.122 M solution in pentane, 1.22 mmol) was added. After a further 30 min stirring, the resulting slightly yellow suspension was filtered through celite, giving a clear yellow solution. This was concentrated *in vacuo* to approximately 10 mL and cooled to −45 °C to afford the product as large yellow crystals. An isolated yield has not been accurately calculated for this thermally unstable compound, but is estimated to be ~50%. **Mass spec.** (EI, *m*/*z*): 540 [Y{**i**}(CH_2SiMe_3)(CH_2SiMe_2)]$^+$, 468 [Y{**i**}(CH_2SiMe_3)]$^+$.

2.6. Synthesis of Y{*i*}(OAr)$_2$ (Ar = 2,6-^{t}Bu$_2$C$_6$H$_3$, **5**)

Heptane (50 mL) was added to a dry mixture of Y(OAr)$_3$ (400 mg, 0.57 mmol) and Li{**i**} (170 mg, 0.57 mmol). The resulting suspension was heated at 85 °C for 3 days. After this time, the suspension was allowed to cool, filtered through celite to remove insoluble LiOAr, and concentrated *in vacuo* to approximately 10 mL. Cooling to −45 °C afforded the product as a white crystalline solid. Isolated yield = 325 mg, 72%. *Anal.* Calc. for $C_{42}H_{64}NO_4Si_2$ (792.04): C, 63.69; H 8.14; N, 1.77. Found: C, 63.89; H, 8.18; N, 1.83%. **^{1}H NMR**: δ 7.29 (d, *J* = 6.0, 4H, *m*-C*H*) 6.82 (t, *J* = 7.5, 2H, *p*-C*H*) 6.21 (d, *J* = 3.0, 2H, furyl-CH_α) 5.61 (m, *J* = 3.0, 2H, furyl-CH_β) 2.22 (s, 6H, furyl-CH_3) 1.41 (s, 36H, CMe_3) 0.34 (s, 12H, SiMe_2). ^{13}C NMR: δ 165.8 (furyl-*C*4) 161.8 (*i*-C_6H_3) 157.2 (furyl-*C*3) 137.9 (*o*-C_6H_3) 126.2 (*m*-C_6H_3) 120.5 (furyl-*C*2) 117.8 (*p*-C_6H_3) 109.0 (furyl-*C*1) 35.4 (*C*Me$_3$) 32.6 (C*Me*$_3$) 15.0 (furyl-CH_3) 5.6 (Si*Me*$_2$).

2.7. Synthesis of Y{*i*}$_2$Cl (**6**)

THF (50 mL) was added to a dry mixture of $YCl_3(THF)_3$ (611 mg, 1.5 mmol) and Li{**i**} (888 mg, 3 mmol) and the resulting slightly yellow solution was stirred at ambient temperature for 48 h. The solvent was removed *in vacuo*. The solid residue was extracted with pentane (50 mL) and filtered through celite to exclude LiCl. The resulting solution was concentrated *in vacuo* to approximately 10 mL, and cooled to −45 °C to afford the product as an off-white crystalline material. Isolated yield 530 mg, 53%. *Anal.* Calc. for $C_{28}H_{44}N_2ClO_4Si_4Y$ (709.36): C, 47.41; H, 6.25; N, 3.95. Found: C, 47.35; H, 6.17; N, 3.90%. **^{1}H NMR**: δ 6.47 (d, *J* = 3.0, 4H, furyl-CH_α) 5.75 (m, *J* = 3.0, 4H, furyl-CH_β) 2.21 (s, 12H, furyl-CH_3) 0.45 (s, 24H, SiMe_2). **^{13}C NMR**: δ 162.4 (furyl-*C*4) 156.9 (furyl-*C*3) 121.4 (furyl-*C*2) 107.8 (furyl-*C*1) 14.2 (furyl-*C*H$_3$) 4.3 (SiMe_2). **Mass spec.** (EI, *m*/*z*): 708 [Y{**i**}$_2$Cl]$^+$.

2.8. Synthesis of Y{*i*}$_2$(CH$_2$Ph) (**7**)

Pre-chilled Et_2O (30 mL) was added to a dry mixture of Y{**i**}$_2$Cl (**6**, 200 mg, 0.28 mmol) and KCH_2Ph (37 mg, 0.28 mmol) and the resulting suspension stirred for 24 h while allowing it to warm up slowly to ambient temperature. Volatiles were removed *in vacuo*, and the pale yellow residue extracted with pentane (40 mL). The extract was filtered through celite to remove KCl. The resulting clear, colourless solution was concentrated *in vacuo* to approximately 5 mL and cooled to −45 °C to afford the product as a pale yellow crystalline material. Isolated yield 100 mg, 46%. *Anal.* Calc. for $C_{35}H_{51}N_2O_4Si_4Y$ (765.04): C, 54.95; H, 6.68; N, 3.67. Found: C, 54.86; H, 6.77; N, 3.80%. **^{1}H NMR**: δ 6.99 (t, *J* = 7.5, 2H, *m*-C_6H_5) 6.72 (t, *J* = 3.0, 1H, *p*-C_6H_5) 6.55 (d, *J* = 6.0, 2H, *o*-C_6H_5) 6.34 (d, *J* = 3.0, 4H, furyl-CH_α) 5.73 (m, *J* = 3.0, 4H, furyl-CH_β) 2.00 (s, 12H, furyl-CH_3) 1.63 (d, *J* = 4.2, 2H, CH_2Ph) 0.43 (s, 24H, SiMe_2). **^{13}C NMR**: δ 164.4 (furyl-*C*4) 156.7 (furyl-*C*3) 129.3, 125.6 (C_6H_5) 121.1 (furyl-*C*2) 120.3 (C_6H_5) 108.4 (furyl-*C*1) 106.1 (C_6H_5) 77.6 (*C*H$_2$Ph) 13.8 (furyl-*C*H$_3$) 5.1 (Si*Me*$_2$). **Mass spec.** (EI, *m*/*z*): 672 [M−CH_2Ph]$^+$.

2.9. Synthesis of [Y{*i*}$_2$][B(C$_6$F$_5$)$_3$(CH$_2$Ph)] (**8**)

C_6D_6 (0.6 mL) was added to a dry mixture of Y{**i**}$_2$(CH_2Ph) (**7**) (30 mg, 0.04 mmol) and $B(C_6F_5)_3$ (20 mg, 0.04 mmol). The resulting solution was left to stand at ambient temperature for 72 h, during which a pale orange oil formed. The solvent was removed *in vacuo* and the residue redissolved in CD_2Cl_2, giving a clear, pale yellow solution. The pure product was isolated by precipitation, by adding the CD_2Cl_2 solution to rapidly stirred pentane (20 mL). The precipitate was isolated as a powder, yield 40 mg (80%). *Anal.* Calc. for $C_{53}H_{51}N_2BF_{15}O_4Si_4Y$ (1277.02): C, 49.85; H, 4.03; N, 2.19. Found: C, 49.78; H, 3.90; N, 2.04%. **^{1}H NMR** (CD_2Cl_2): δ 6.97 (d, *J* = 3.0, 4H, furyl-CH_α) 6.70, 6.90 (overlapping multiplet, 5H, C_6H_5) 6.32 (m, *J* = 3.0, 4H, furyl-CH_β) 2.83 (br s, 2H, CH_2Ph) 2.15 (s, 12H, furyl-CH_3) 0.21 (s, 24H, SiMe_2).

2.10. X-ray data

Details of the crystal data, intensity collection and refinement for complexes [**1**]$_2$, **2** and **3** are collected in Table 1, and for **4**, **5**, [**6**]$_2$ and **7** in Table 5. Crystals were covered in an inert oil and suitable single crystals were selected under a microscope and mounted on a Kappa CCD diffractometer. The structures were refined with SHELXL-97 [20]. Details specific to individual datasets are outlined below:

[Sc{i}Cl$_2$]$_2$ ([**1**]$_2$): there are two molecules of toluene solvate in the lattice.

Sc{i}(OAr)$_2$ (**3**): there are two independent molecules in the unit cell that differ slightly in their bond lengths and angles.

Y{i}(CH$_2$SiMe$_3$)$_2$(THF)$_2$ (**4**): the molecule lies on a crystallographic twofold rotation axis.

Y{i}(OAr)$_2$ (**5**): the C(35) ^{t}Bu group is disordered over two positions; the lower occupancy methyl C atom sites were left isotropic.

Y{i}$_2$(CH$_2$Ph) (**7**): there are two independent molecules in the unit cell that differ slightly in their bond lengths and angles.

2.11. Screening for olefin polymerization activity

A 500 mL round bottom flask fitted with a dreschel head was purged with argon and rinsed with a solution of DIBAL in hexane (10 mL of a 1.0 M solution). A small amount of the DIBAL solution remained in the flask during the polymerization procedure. A solution of the precatalyst compound in toluene (50 mL) was then added, followed by a solution of the relevant co-catalyst compound in toluene (50 mL). Additional toluene was added to make the total volume between 150 and 200 mL. Ethylene gas was bubbled through the flask at atmospheric pressure with rapid stirring. After 60 min, the gas flow was halted, the contents of the flask exposed to the atmosphere, and 100 mL of methanol was added to quench the reaction. The solid polymer was collected by filtration and dried under reduced pressure at a temperature of 160 °C for 12 h. The activity was calculated from the mass of dry polymer obtained.

2.12. Sample preparation for GPC analysis

A single solution of each sample was prepared by adding 15 mL of solvent to 15 mg of sample. All of the solutions were heated, with shaking, for 60 min at 190 °C. Solutions were filtered at 160 °C through a glass fibre pad, and part of each of the filtered solution was transferred to glass sample vials. The vials were placed in a heated sample compartment and after an initial delay of 30 min, to allow the samples to equilibrate thermally; injection of part of the contents of each vial was carried out.

Table 1
Crystal structure and refinement data for [Sc{**i**}Cl$_2$]$_2$ ([**1**]$_2$),.Sc{**i**}(CH$_2$SiMe$_3$)$_2$ (**2**) and Sc{**i**}(OAr)$_2$ (Ar = 2,6-^{t}Bu$_2$C$_6$H$_2$, **3**).

	[**1**]$_2$	**2**	**3**
Formula	$C_{28}H_{44}Cl_4N_2O_4Sc_2Si_4{\cdot}2(C_7H_8)$	$C_{22}H_{44}NO_2ScSi_4$	$C_{42}H_{64}NO_4ScSi_2$
Formula weight	1001.00	511.90	748.08
T (K)	173(2)	173(2)	173(2)
Wavelength (Å)	0.71073	0.71073	0.71073
Crystal size (mm)	0.15 × 0.15 × 0.10	0.30 × 0.30 × 0.30	0.20 × 0.20 × 0.05
Crystal system	monoclinic	monoclinic	orthorhombic
Space group	$P2_1/c$ (No. 14)	$P2_1/c$ (No. 14)	$Pca2_1$ (No. 29)
a (Å)	10.6042(5)	11.6836(2)	19.3368(2)
b (Å)	15.3248(7)	15.9080(3)	11.3263(1)
c (Å)	16.3082(7)	16.7379(3)	39.1369(4)
β (°)	101.569(3)	91.209(1)	90
V (Å^3)	2596.4(2)	3110.26(10)	8571.54(15)
Z	2	4	8
D_c (Mg m^{-3})	1.28	1.09	1.16
Absorption coefficient (mm^{-1})	0.60	0.41	0.27
θ Range for data collection (°)	3.40–26.01	3.49–26.00	3.47–26.02
Reflections collected	16 582	38 184	54 063
Independent reflections [$R_{(int)}$]	5070 [0.065]	6099 [0.045]	14 732 [0.045]
Reflections with $I > 2\sigma(I)$	3294	5187	12 029
Data/restraints/parameters	5070/0/264	6099/0/273	14 732/1/938
Goodness-of-fit (GOF) on F^2	1.011	1.020	1.019
Final R indices [$I > 2\sigma(I)$]	R_1 = 0.050, wR_2 = 0.091	R_1 = 0.032, wR_2 = 0.078	R_1 = 0.041, wR_2 = 0.087
R indices (all data)	R_1 = 0.097, wR_2 = 0.106	R_1 = 0.042, wR_2 = 0.083	R_1 = 0.060, wR_2 = 0.095
Largest difference peak/hole (e Å^{-3})	0.29 and −0.34	0.29 and −0.24	0.22 and −0.24

3. Results and discussion

3.1. Mono-amide scandium compounds

Salt metathesis between $ScCl_3$ or $ScCl_3(THF)_3$ and a stoichiometric quantity of Li{**i**} in THF affords the base-free, mono ligand compound, Sc{**i**}Cl$_2$ (**1**) after extraction and crystallisation from toluene (Scheme 1). The long reaction time (5 days) was required to maximise the yield, as performing the synthesis without heating or for less time gave a lower quantity of **1** that was contaminated with unreacted Li{**i**}. The compound was isolated as colourless crystals that showed a single environment for each of the furyl groups by ^{1}H and ^{13}C NMR spectroscopy, consistent with static **A**- or **C**-type bonding, or a rapid exchange of groups in **B**-type ligation.

Treatment of $ScCl_3(THF)_3$ with two equivalents of Li{**i**} under prolonged reflux in THF did not result in isolation of the corresponding *bis*-amido complex, Sc{**i**}$_2$Cl. This contrasts with the chemistry of titanium,as Ti{**i**}$_2$Cl and Ti{**i**}$_2$Cl$_2$ can be readily synthesized from the Ti(III) or Ti(IV) chloride, respectively, using two equivalents of Li{**i**} at ambient temperature [12]. The small size of the scandium metal is unlikely to be a factor, since the ionic radius [21] of Sc^{3+} (0.73 Å) compares favourably with Ti^{3+} (0.76 Å) and Ti^{4+} (0.68 Å). The lower solubility of the scandium compounds may therefore be a factor in limiting the complexation to a single equivalent of {**i**}, although we cannot rule out the formation of [Sc{**i**}$_2$Cl$_2$]Li during the course of this reaction.

The molecular structure of **1** was solved by single crystal X-ray diffraction (Fig. 3, and Tables 1 and 2). The amido ligand {**i**} binds with **C**-type coordination, generating a twist angle, α, of 11.07° between the two 'ScNSiCO' metallacycles. A similar bonding mode was observed in the aluminium complex, Al{**i**}Cl$_2$ [13], although ultimately in this case a five-coordinate aluminium(III) was formed, rather than the distorted octahedral scandium centres in **1** that result from formation of the μ,μ′-dichlorobridged dimer, [**1**]$_2$. The Sc–N distance [2.038(2) Å] is identical to that found in the five-coordinate amido-compound Sc(N{SiMe$_3$}$_2$)Cl$_2$(THF)$_2$ (**a**) [2.039(2) Å] [22], but notably shorter than in the octahedral compound Sc(N{SiMe$_2$CH$_2$P^{i}Pr$_2$}$_2$)Cl$_2$(THF) (**b**) [2.101(7) Å] [23]. The Sc–O$_{furyl}$ bond lengths in [**1**]$_2$ [2.274(2) Å and 2.281(2) Å] are longer than the Sc–O$_{THF}$ distances in **a** [2.176(2) Å and 2.175(2) Å], but comparable to those in **b** [2.271(7) Å]. Significant differences in Sc–Cl bond length between terminal and bridging chlorides [Δ_{Sc-Cl} (max): 0.20 Å in [**1**]$_2$] have been noted elsewhere [23,24]. It is curious to note the monomeric formulation of the metal in both **a** and **b**, with incorporation of THF in the coordination sphere of scandium. Despite carrying out syntheses of **1** in THF, or employing

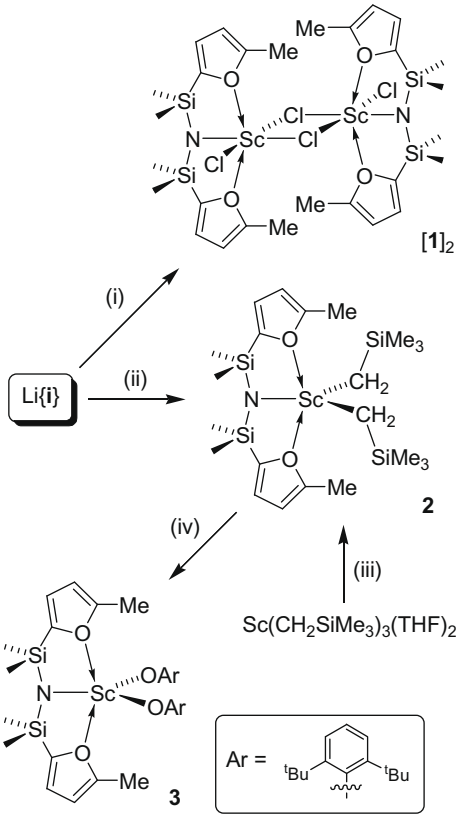

Scheme 1. Synthetic route to scandium compounds incorporating {**i**}: (i) $ScCl_3$ or $ScCl_3(THF)_3$; (ii) $ScCl_3(THF)_3$, 2 $LiCH_2SiMe_2$ (one-pot); (iii) H{**i**}; (iv) 2 HOAr (Ar = 2,6-^{t}Bu$_2$C$_6$H$_3$).

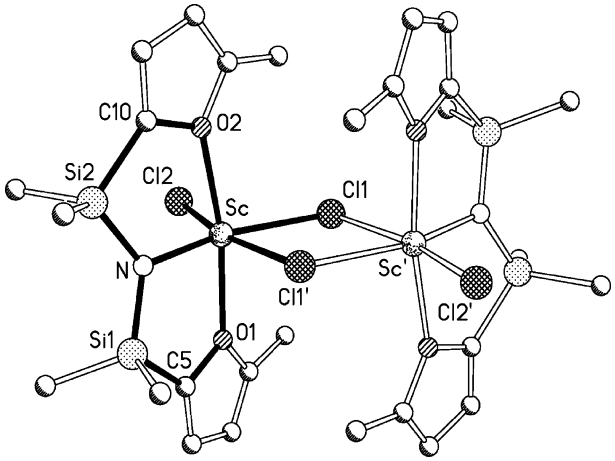

Fig. 3. Molecular structure of $[\mathbf{1}]_2$ with hydrogen atoms and toluene solvate omitted.

Table 2
Selected bond lengths (Å) and angles (°) for $[Sc\{\mathbf{i}\}Cl_2]_2$ ($[\mathbf{1}]_2$).

Sc–N	2.038(2)	Sc–Cl1	2.5607(9)
Sc–O1	2.274(2)	Sc–Cl2	2.3804(10)
Sc–O2	2.281(2)	Sc–Cl1′	2.5813(9)
N–Si1	1.713(2)	N–Si2	1.708(2)
N–Sc–O1	84.70(8)	N–Sc–O2	86.04(8)
N–Sc–Cl2	106.25(7)	N–Sc–Cl1′	87.31(7)
Cl1–Sc–Cl2	90.63(3)	Cl–Sc–Cl1′	75.84(3)
O1–Sc–Cl1	92.08(5)	O1–Sc–Cl1′	90.44(6)
O1–Sc–Cl2	90.93(6)	O2–Sc–Cl1	97.84(5)
O2–Sc–Cl1′	92.78(6)	O2–Sc–Cl2	88.15(6)
Sc–Cl1–Sc′	104.16(3)	Sc–N–Si1	118.44(12)
Sc–N–Si2	117.96(12)	Si1–N–Si2	123.35(14)

$ScCl_3(THF)_3$ as the starting reagent, formation of the dimer is preferred over the solvated monomer, contrasting with Okuda's furyl-substituted Cp system, $Sc(\eta\text{-}C_5Me_4SiMe_2R)(CH_2SiMe_3)_2(THF)$ (R = furyl, 2-methylfuryl) in which the furyl-group is non-coordinating in the solid-state [25].

Reaction of **1** with the alkyl-lithium reagents LiMe and $LiCH_2SiMe_3$ resulted in ligand transfer of {**i**} from Sc to Li, affording the lithium amide salt Li{**i**} [11]. This mode of reactivity has previously been documented for the titanium compound $Ti\{\mathbf{i}\}_2Cl_2$, where it was rationalized in terms of interaction of a non-coordinated furyl group (the solid-state structure of $Ti\{\mathbf{i}\}_2Cl_2$ displayed **B**-type bonding) with the lithium centre. Reaction of **1** with KCH_2Ph in diethyl ether also results in ligand transfer to afford the potassium amide salt K{**i**} [11].

An alternative pathway to organometallic scandium compounds is alkane elimination using $Sc(CH_2SiMe_3)_3(THF)_2$ as a convenient metal reagent [26]. The *tris*-alkyl precursor can be prepared *in situ* from the reaction of three equivalents of $LiCH_2SiMe_3$ with $ScCl_3(THF)_3$ in pentane at −78 °C [16,27]. In our study, alkane elimination proceeded smoothly using the free amine H{**i**}, to form the scandium dialkyl, $Sc\{\mathbf{i}\}(CH_2SiMe_3)_2$ (**2**) with concomitant formation of $SiMe_4$ (Scheme 1). Alternatively, **2** was prepared in a 'one-pot' procedure combining $ScCl_3(THF)_3$ with one equivalent of Li{**i**} and two equivalents of $LiCH_2SiMe_3$ at −78 °C. Identical isolated yields of 50% were obtained in each case.

Formulation of **2** as the base-free compound was confirmed by ^1H and ^{13}C NMR spectroscopy and elemental analysis. As for **1**, NMR indicates a symmetrically bound amide ligand, with singlet resonances for both proton environments of the alkyl groups. Compound **2** is surprisingly stable for a scandium dialkyl compound. It is thermally robust and can be stored in the solid-state at ambient temperature. It failed to react further when exposed to additional H{**i**}, even at elevated temperatures, and is also unreactive towards hydrogen gas, even at high pressure for an extended period of time (10 bar for 5 days).

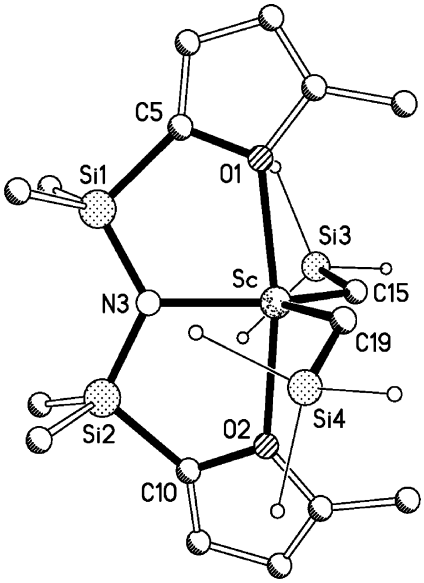

Fig. 4. Molecular structure of **2** with hydrogen atoms omitted and methyl groups of the alkyl ligands reduced in size.

Table 3
Selected bond lengths (Å) and angles (°) for $Sc\{\mathbf{i}\}(CH_2SiMe_3)_2$ (**2**).

Sc–N3	2.0934(13)	Sc–C15	2.2324(18)
Sc–C19	2.2137(17)	Sc–O1	2.2745(11)
Sc–O2	2.2942(12)	N3–Si1	1.7035(14)
N3–Si2	1.7073(14)	Si3–C15	1.8374(19)
Si3–C16	1.882(2)	Si3–C17	1.866(2)
Si3–C18	1.869(2)	Si4–C19	1.8379(17)
Si4–C20	1.871(2)	Si4–C21	1.872(2)
Si4–C22	1.873(2)		
N3–Sc–C15	122.93(6)	N3–Sc–C19	122.69(6)
C15–Sc–C19	114.33(7)	O1–Sc–N3	84.37(5)
O1–Sc–C15	94.00(6)	O1–Sc–C19	94.28(6)
O2–Sc–N3	85.31(5)	O2–Sc–C15	90.80(6)
O2–Sc–C19	92.08(6)	O1–Sc–O2	169.64(4)
Sc–C15–Si3	121.18(9)	Sc–C19–Si4	126.82(9)

The molecular structure of **2** (Fig. 4, and Tables 1 and 3) is monomeric with ligand {**i**} bound with **C**-type coordination at a distorted trigonal bipyramidal metal ($\tau = 0.78$ [28], $\alpha = 6.55°$) in which the furyl substituents are located in axial positions. Unusually for *bis*-alkyl Sc compounds incorporating co-planar CH_2SiMe_3 ligands, the two $SiMe_3$ groups are projected away from one another (**c**, Fig. 5) rather than being present in the staggered conformation (**d**) exemplified by the $Sc(\eta\text{-}C_5R_5)(CH_2SiMe_3)_2(THF)$ series of compounds[1] [29,30]. This is a likely consequence of the methyl substituents from the furyl groups occupying space directly above and below the equatorial plane of the tbp metal. The Sc–N bond [2.0934(14) Å] is slightly longer than in $[\mathbf{1}]_2$ reflecting the increased electron density at scandium due to the presence of the alkyl ligands. The average Sc–C bond length [2.2231(18) Å] is in the range previously observed for 5-coordinate '$Sc(CH_2SiMe_3)_2$' fragments [23,31–40].

[1] Conformation **e** is strongly disfavoured for in-plane alkyl groups on simple steric considerations.

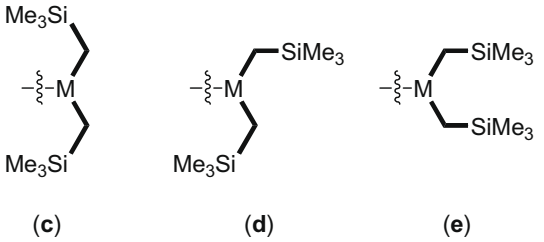

Fig. 5. Three possible conformations of two trimethylsilylmethyl ligands in a tbp geometry with equatorial alkyl groups.

Closer inspection of the bond parameters associated with the two alkyl groups indicates a degree of asymmetry. One of the Sc–C bonds is slightly but significantly longer than the other [Sc–C15 2.2324(18) Å; Sc–C19 2.2137(17) Å], accompanied by a reduced Sc–C–Si angle [121.18(9)° versus 126.82(9)°]. The silicon atom of this ligand (Si3) is displaced by 0.24 Å from the $NScC_2$ equatorial plane, whereas Si4 is located at a distance of 0.77 Å. Given the high Lewis acidity predicted for the metal in **2** (formal electron count of 12 e^-) and the coordinative unsaturation of the scandium, it is not unreasonable to expect α-agostic interactions with the methylene hydrogen atoms [41]. However, given the lack of additional experimental evidence, we are reluctant to invoke such an explanation for the observed asymmetry in alkyl bonding, particularly given the likelihood of dominant steric factors involving the bulky trimethylsilylmethyl ligands and furyl substituents of {**i**} present in **2**.

The alkyl-ligands in **2** react selectively with HOAr (Ar = 2, 6-^{t}Bu$_2$C$_6$H$_3$) with retention of ligand {**i**}, in a procedure analogous to that for the TACN-substituted compound Sc($O_{Ar}N_3$)(CH_2SiMe_3)$_2$ [$O_{Ar}N_3$ = 2,4-^{t}Bu$_2$C$_6$H$_2$O-CH_2-4,7-Me_2TACN] [42], and the tris(pyrazolyl)methane compound Sc(CH_2SiMe_3)$_3$(HC{Me_2pz}$_3$) [43]. Reaction of **2** with two equivalents of HOAr cleanly forms the scandium bis-aryloxide compound, Sc{**i**}(OAr)$_2$ (**3**) with elimination of $SiMe_4$ (Scheme 1). NMR data are consistent with a product in which the amide is symmetrically bound and the two aryloxide groups are equivalent.

The molecular structure of **3** was solved by single crystal X-ray diffraction (Fig. 6, and Tables 1 and 4). There are two molecules in the unit cell that differ slightly in bond lengths and angles; parameters for the second molecule are presented {*thus*}. As in **2**, the metal is five-coordinate with **C**-type bonding involving both furyl substituents and a twist angle α of 19.99° {20.43°}). Examination of the coordination geometry in **3**, however, shows that it is best described as a distorted square-based pyramid (τ = 0.28 {0.29}) with the basal plane described by N1 O1 O2 O3 [Sc located 0.74 Å {0.85 Å} above this plane], and the O4-aryloxide group in the apical position. The Sc–N bond length [2.100(3) Å {2.092(2) Å}] is comparable to that found in **2**, although there is a notable contraction of the Sc–O_{furyl} distances. The Sc–$O_{aryloxide}$ distances are essentially equivalent, despite the different geometric locations within the square-based pyramid, and are within the range found for other terminal aryloxides of scandium [19,42–45]. The angles at $O_{aryloxide}$ are close to linear, also common for this type of linkage at scandium. The C_6-ring of the basal aryloxide is rotated to be approximately perpendicular to the O_3N-plane [angle between mean planes = 85.09° {85.27°}], with the corresponding ring of the apical ligand approximately parallel with the O_{furyl}–Sc–O_{furyl} vector [angle between mean planes = 17.70° {13.94°}].

3.2. Mono-amide yttrium compounds

In contrast to the clean synthesis of **1**, the stoichiometric reaction between $YCl_3(THF)_3$ and Li{**i**} in THF invariably lead to a mixture of products that could not be separated by fractional crystallisation or sublimation. To circumvent this problem and access mono-amide compounds, the reaction between H{**i**} and Y(CH_2SiMe_3)$_3$(THF)$_2$ (generated *in situ*) was performed in an analogous procedure to the preparation of **2** (Scheme 2). The isolated yellow crystals, **4**, were unstable, and decomposed within 12 h at room temperature. As a consequence, reliable NMR spectra have not been recorded and elemental analysis is unavailable. However, single crystal X-ray diffraction has been performed on a representative crystal of **4**, confirming the formulation as the solvated *bis*-alkyl, Y{**i**}(CH_2SiMe_3)$_2$(THF)$_2$.

The molecular structure of **4** (Fig. 7, and Tables 5 and 6) shows a trigonal bipyramidal yttrium in which, contrasting with the base-free scandium derivative Sc{**i**}(CH_2SiMe_3)$_2$ (**2**) the amide ligand {**i**} is present with **A**-type coordination with neither of the furyl groups associated with the metal. Instead, two molecules of THF complete the coordination sphere as the axial ligands, with a resultant τ value of 0.82. The preference for THF coordination in the presence of the potentially chelating furyl groups has previously been observed with {**i**} in the structurally characterized aluminium complex, Al{**i**}Cl_2(THF) [13].

There are few other structurally characterized examples of *bis*-trimethylsilylmethyl complexes of yttrium containing terminal amide groups with which to compare the structure of **4** [46], with

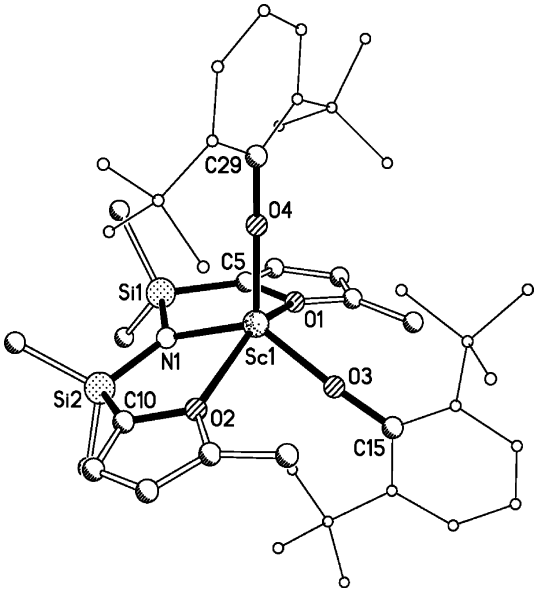

Fig. 6. Molecular structure of one of the independent molecules of **3** with hydrogen atoms omitted and aryl substituents reduced in size.

Table 4
Selected bond lengths (Å) and angles (°) for Sc{i}(OAr)$_2$ (3) {molecule 2}.

Sc1–N1	2.100(3) {2.092(2)}	Sc1–O1	2.357(2) {2.356(2)}
Sc1–O2	2.432(2) {2.435(2)}	Sc1–O3	1.934(2) {1.935(2)}
Sc1–O4	1.937(2) {1.934(2)}	N1–Si1	1.711(3) {1.715(3)}
N1–Si2	1.703(3) {1.705(2)}	O3–C15	1.355(3) {1.357(3)}
O4–C29	1.366(4) {1.375(4)}		
N1–Sc1–O3	131.45(10) {130.60(10)}	N1–Sc1–O4	107.90(10) {106.87(10)}
O3–Sc1–O4	120.57(9) {122.43(9)}	O1–Sc1–N1	81.10(9) {81.24(8)}
O1–Sc1–O3	88.70(8) {88.32(8)}	O1–Sc1–O4	98.80(8) {98.42(8)}
O2–Sc1–N1	81.10(9) {81.10(9)}	O2–Sc1–O3	83.55(8) {83.25(8)}
O2–Sc1–O4	111.81(8) {112.15(8)}	O1–Sc1–O2	148.09(8) {148.02(8)}
Sc1–O3–C15	172.16(18) {172.10(18)}	Sc1–O4–C29	172.88(19) {170.0(2)}

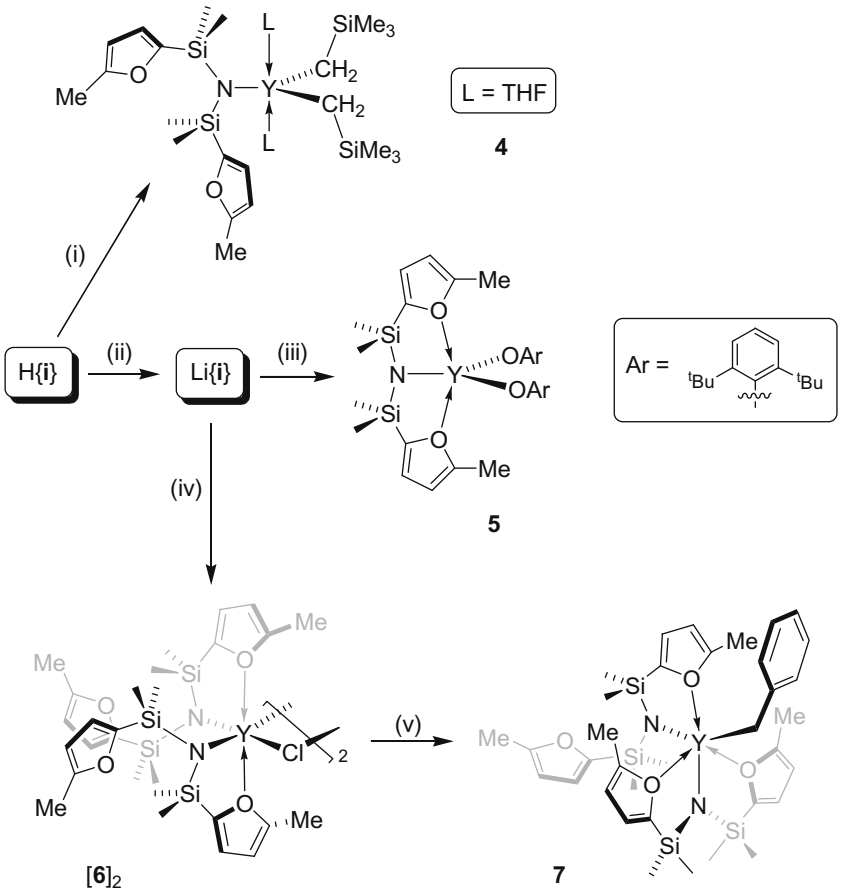

Scheme 2. (i) $Y(CH_2SiMe_3)_3(THF)_2$ (in situ); (ii) ^nBuLi; (iii) $Y(OAr)_3$; (iv) 0.5 $YCl_3(THF)_3$; (v) KCH_2Ph.

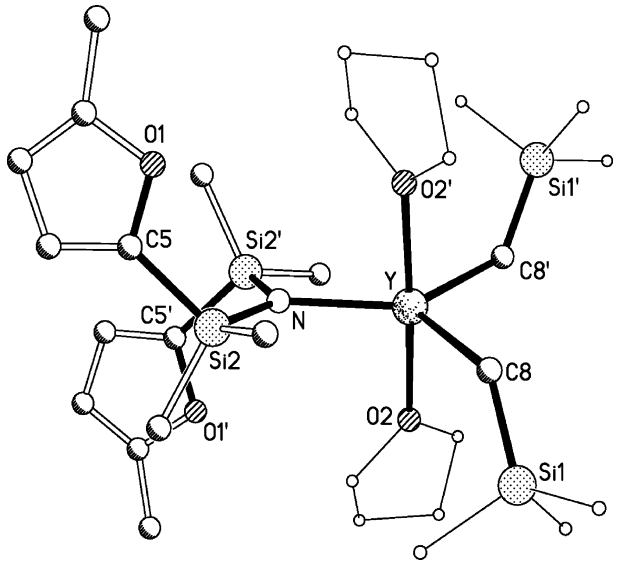

Fig. 7. Molecular structure of **4** (′ = $-x$, y, $-z+3/2$) with hydrogen atoms omitted and methyl groups of the alkyl ligands and methylene groups of THF reduced in size.

the field dominated by amides incorporating additional donor interactions, as in amino-phosphine ligands [47], and *N*,*N*′-chelating ligands such as amidinates/guanidinates [48–52], or β-diketiminates [53,54]. The Y–N bond length [2.290(3) Å] is within the range found for other five-coordinate yttrium compounds with terminal amides [55–57], with a Y–C bond length also typical for this linkage. Comparing the conformation of the alkyl groups with the scandium complex **2**, we note that the silyl groups are now twisted such that Si1 is located 1.33 Å out of the YNC_2 equatorial plane. This is possible in **4** as the replacement of the furyl groups with THF molecules in the metal coordination sphere removes the methyl substituents C1 and C14 that were directing the $SiMe_3$ groups (Fig. 8) in addition to allowing an increased O–M–O angle [169.64(4)° M = Sc; 177.27(9)° M = Y].

An attempt was made to synthesise a similar yttrium dialkyl compound using the more bulky, base-free yttrium tris-alkyl precursor $Y(CH\{SiMe_3\}_2)_3$, where the bulk of the bis-trimethylsilylmethyl group was predicted to make incorporation of solvent molecules into the final complex less likely. Unfortunately, the free amine H{**i**} failed to react with this hindered yttrium tris-alkyl, even at elevated temperatures for prolonged reaction times.

It has been shown previously that $Y(OAr)_3$ is susceptible to salt metathesis with $LiCH(SiMe_3)_2$ in hexane, affording base-free yttrium *tris*-alkyl compounds [58]. The LiOAr side-product is insoluble in the reaction solvent, enabling easy separation of the product by filtration. As an alternative route to access mono-amide complexes of {**i**}, $Y(OAr)_3$ was therefore reacted with one equivalent of Li{**i**}, affording Y{**i**}$(OAr)_2$ (**5**) as colourless crystals. Forcing conditions are required for this reaction to go to completion (reflux, 3 days) but the product is thermally stable and can be obtained in 72% isolated yield. ^1H and ^{13}C NMR spectroscopy and elemental analysis were consistent with **5** being closely related to the scandium analogue.

Single crystal X-ray diffraction confirmed **5** as the base-free five-coordinate compound with **C**-type bonding for the amide

Table 5
Crystal structure and refinement data for Y{**i**}$(CH_2SiMe_3)_2(THF)_2$ (**4**), Y{**i**}$(OAr)_2$ (Ar = 2,6-^{t}Bu$_2$C$_6$H$_2$, **5**), [Y{**i**}$_2$Cl]$_2$ ([**6**]$_2$) and Y{**i**}$_2CH_2Ph$ (**7**).

	4	**5**	[**6**]$_2$	**7**
Formula	$C_{30}H_{60}NO_4Si_4Y$	$C_{42}H_{64}NO_4Si_2Y$	$C_{56}H_{88}Cl_2N_4O_8Si_8Y_2$	$C_{35}H_{51}N_2O_4Si_4Y$
Formula weight	700.06	792.03	1418.74	765.05
T (K)	173(2)	173(2)	173(2)	173(2)
Wavelength (Å)	0.71073	0.71073	0.71073	0.71073
Crystal size (mm)	0.35 × 0.35 × 0.30	0.35 × 0.30 × 0.30	0.40 × 0.30 × 0.25	0.30 × 0.30 × 0.20
Crystal system	monoclinic	monoclinic	triclinic	triclinic
Space group	$C2/c$ (No. 15)	$P2_1/n$ (No. 14)	$P\bar{1}$ (No. 2)	$P\bar{1}$ (No. 2)
a (Å)	18.2436(5)	16.4471(3)	14.1280(2)	12.1725(2)
b (Å)	11.3155(4)	14.7478(3)	15.5378(2)	18.9507(5)
c (Å)	20.8494(6)	18.2103(3)	18.5487(3)	19.3590(4)
α (°)	90	90	69.760(1)	115.703(1)
β (°)	111.939(2)	102.113(1)	88.309(1)	90.106(1)
γ (°)	90	90	70.072(1)	98.532(1)
V (Å^3)	3992.4(2)	4318.72(14)	3573.51	3968.29(15)
Z	4	4	2	4
D_c (Mg m^{-3})	1.17	1.22	1.32	1.28
Absorption coefficient (mm^{-1})	1.61	1.44	1.87	1.63
θ Range for data collection (°)	3.44–25.94	3.40–26.03	3.40–26.04	3.41–26.01
Reflections collected	18 784	56 818	57 091	58 828
Independent reflections [$R_{(int)}$]	3884 [0.044]	8493 [0.060]	14 068 [0.052]	15 525 [0.052]
Reflections with $I > 2\sigma(I)$	3388	6785	11 085	11 791
Data/restraints/parameters	3884/0/183	8493/0/466	14 068/0/729	15 525/0/837
Goodness-of-fit (GOF) on F^2	0.602	1.027	1.005	1.034
Final R indices [$I > 2\sigma(I)$]	R_1 = 0.033, wR_2 = 0.102	R_1 = 0.041, wR_2 = 0.081	R_1 = 0.038, wR_2 = 0.075	R_1 = 0.044, wR_2 = 0.085
R indices (all data)	R_1 = 0.043, wR_2 = 0.116	R_1 = 0.061, wR_2 = 0.087	R_1 = 0.059, wR_2 = 0.083	R_1 = 0.072, wR_2 = 0.094
Largest difference peak/hole (e Å^{-3})	0.34 and −0.27	0.28 and −0.29	0.39 and −0.46	0.68 and −0.32

Table 6
Selected bond lengths (Å) and angles (°) for Y{**i**}$(CH_2SiMe_3)_2(THF)_2$ (**4**).

Y–N	2.290(3)	Y–C8	2.403(3)
Y–O2	2.374(2)	N–Si2	1.713(2)
Si1–C8	1.836(3)	Si1–C9	1.872(3)
Si1–C10	1.868(3)	Si1–C11	1.882(3)
N–Y–C8	127.94(7)	N–Y–O2	88.64(4)
C8–Y–C8′	104.12(15)	O2–Y–C8	95.20(9)
O2′–Y–C8	86.48(9)	O2–Y–O2′	177.27(9)
Y–C8–Si1	132.39(15)		

(Fig. 9, and Tables 5 and 7). Although not isomorphous with the scandium analogue [**3** = orthorhombic, **5** = monoclinic], the gross structural features of **5** are similar, with the metal best described as distorted square pyramidal, with a τ value of 0.38 and O3 located in the apical position. The Y–N distance [2.250(2) Å] is slightly less than in **4** reflecting the more electron deficient metal and the Y–O bond lengths [2.0891(16) Å and 2.0887(16) Å] are in the range previously observed for terminal aryloxides of yttrium [59–62].

In contrast to the reported preparation of Y$(CH\{SiMe_3\}_2)_3$ that proceeds *via* displacement of all three aryloxide ligands from Y$(OAr)_3$ with LiCH$(SiMe_3)_2$ at ambient temperature in 30 min [58], further reaction of Y{**i**}$(OAr)_2$ with alkyl-lithium reagents was unsuccessful, even at elevated temperatures. It was similarly unreactive towards the alkyl-potassium reagents KCH_2Ph or KCH_2SiMe_3. We attribute this lack of reactivity to the bulk of the aryl oxides and the retention of the bound furyl groups in solution, thereby preventing access of any substrates to the metal centre.

3.3. Bis-amide yttrium compounds

Although it did not prove possible to coordinate more than one equivalent of amide {**i**} at scandium (*vide supra*) the metathesis reaction between $YCl_3(THF)_3$ and two equivalents of Li{**i**} afforded the *bis*-amide, Y{**i**}$_2$Cl (**6**) in reasonable isolated yield (Scheme 2). Elemental analysis was consistent with a base-free compound of formulation Y{**i**}$_2$Cl that did not retain THF at yttrium, and the highest molecular weight peak in the mass spec was consistent with monomeric [Y{**i**}$_2$Cl]$^+$ (m/z = 708). ^{1}H and ^{13}C NMR spectroscopy showed a single environment for each of the furyl groups, which if a static structure was evident in solution, would qualify as a 3-coordinate metal (**A**-type bonding) or a 7-coordinate metal (**C**-type bonding). Whilst examples of 3-coordinate yttrium compounds involving terminal amides have been structurally characterized [57,63], 7-coordinate examples are have not been reported. An alternative explanation, therefore, is a fluxional system in solution with **B**-type bonding, which would render each amide bidentate, generating a more reasonable 5-coordinate geometry at yttrium.

In fact, the molecular structure of Y{**i**}$_2$Cl was shown by X-ray crystallography to be the μ,μ′-dichlorobridged dimer, [**6**]$_2$, with distorted octahedral yttrium metal centres (Fig. 10, and Tables 5 and 8). Each yttrium is crystallographically distinct, with *cis*-nitrogen and *trans*-furyl groups and angles in the range 108.40(7)–72.539(19)° and 108.23(7)–73.246(19)° for Y1 and Y2, respectively. As predicted, each of the ligands adopts a **B**-type coordination at yttrium in which only one of the furyl substituents binds to the metal. The central Y_2Cl_2 component of [**6**]$_2$ is planar (max deviation 0.02 Å) with a pronounced twist of each N–Y–N plane relative to this plane [Y1, 12.04°; Y2, 15.22°].

Treatment of **6** with KCH_2Ph at −78 °C afforded the yttrium mono-benzyl compound Y{**i**}$_2(CH_2Ph)$ (**7**) in 46% isolated yield. This result is in contrast to previous attempts to alkylate group 3 (or group 4 [12]) compounds containing {**i**} with lithium-alkyl or potassium-alkyl reagents, where a common mode of activity was ligand transfer and formation of Li{**i**} or K{**i**}. ^{1}H NMR spectra show a single symmetric species in solution, with a coupling constant 4.2 Hz between the ^{89}Y and the methylene protons of the benzyl ligand.

Single crystal X-ray diffraction of **7** (Fig. 11, and Tables 5 and 9) showed the molecular structure to be monomeric, with one of the yttrium bound amides having a **B**-type coordination mode and the other a **C**-type with α = 19.35° {17.29°}. The resultant six-coordinate complex is best described as trigonal prismatic (Fig. 12) in

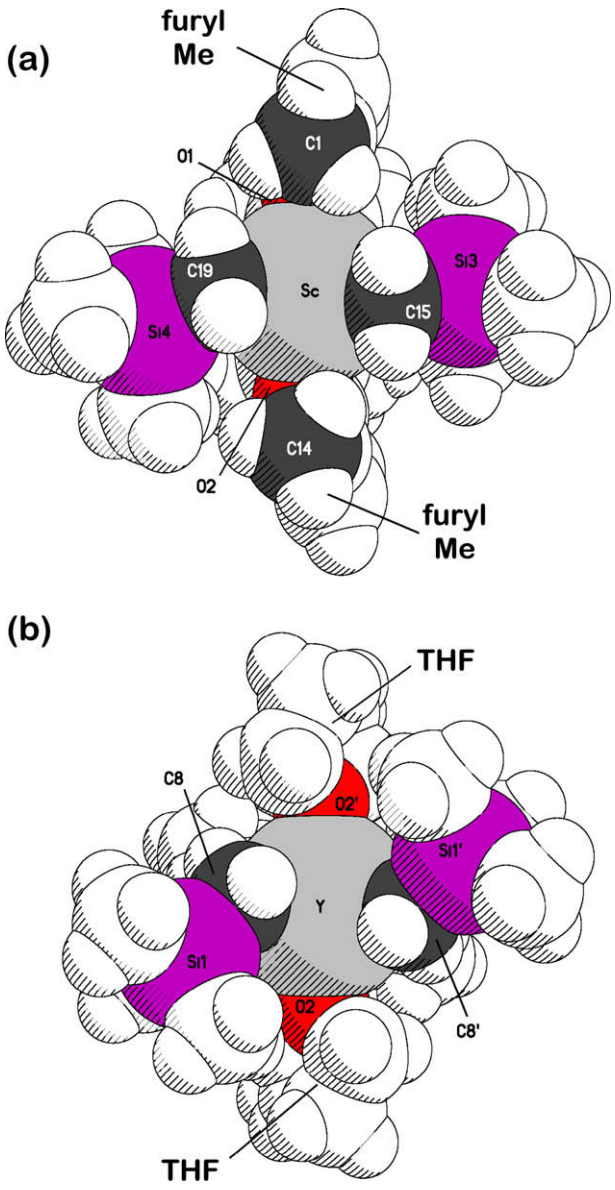

Fig. 8. Space filling representation of bis-alkyls (a) **2** and (b) **4**, viewed along the M–N bond showing the influence of the furyl-Me substituents on the $SiMe_3$ groups.

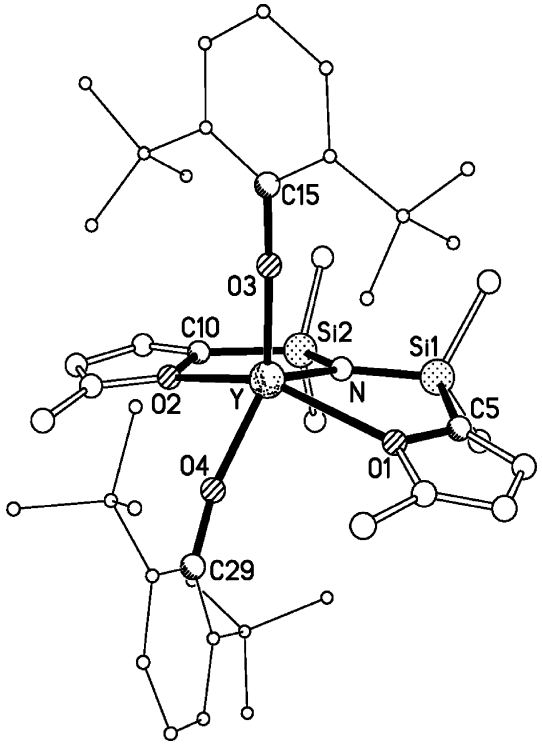

Fig. 9. Molecular structure of **5** with hydrogen atoms omitted and aryl substituents reduced in size.

Table 7
Selected bond lengths (Å) and angles (°) for Y{**i**}$(OAr)_2$ (**5**).

Y–N	2.250(2)	Y–O1	2.4863(16)
Y–O2	2.4845(16)	Y–O3	2.0891(16)
Y–O4	2.0887(16)	N–Si1	1.702(2)
N–Si2	1.704(2)	O3–C15	1.361(3)
O4–C29	1.352(3)		
N–Y–O3	108.74(7)	N–Y–O4	124.37(7)
O3–Y–O4	126.55(6)	O1–Y–N	79.03(6)
O1–Y–O3	99.85(6)	O1–Y–O4	85.59(6)
O2–Y–N	80.14(6)	O2–Y–O3	110.53(6)
O2–Y–O4	85.75(6)	O1–Y–O2	147.36(6)
Y–O3–C15	175.10(15)	Y–O4–C29	166.42(15)

which the benzyl methylene group and the *N*,*O*-component of the **C**-type amide define one face, with the remaining *O*-atom of the furyl group from the **C**-amide combining with the *N*- and *O*-bonding atoms of the **B**-type ligand {**i**} to form the opposite face. The two triangular faces are roughly parallel (angle between planes = 7.78° {8.35°}) although there is a displacement of the two faces such that the interplanar angle at the vertices ranges between 76.59° (N2···O1···N1) to 109.18° (O2···N1···O1) {corresponding angles in second molecule: 76.41–109.37°}.

Structurally characterized yttrium benzyls remain scarce in the literature [48,64–66], with the only other diamide involving the bulky chelating ligand set, $[ArN(CH_2)_3NAr]^{2-}$ (Ar = 2,6-^{i}Pr$_2$C$_6$H$_3$) [67]. The Y–C bond length in **7** [2.420(3) Å {2.422(2) Å}] is towards the short end of the range found for this linkage, and the angle at the methylene carbon [119.2(2)° {120.3(2)°}] is indicative of a η^1-bound benzyl group. The Y1–O1 distance [2.703(2) Å {2.691(2) Å}] is significantly longer than to the other furyl oxygen atoms, suggesting a weak interaction that would be easily broken in solution.

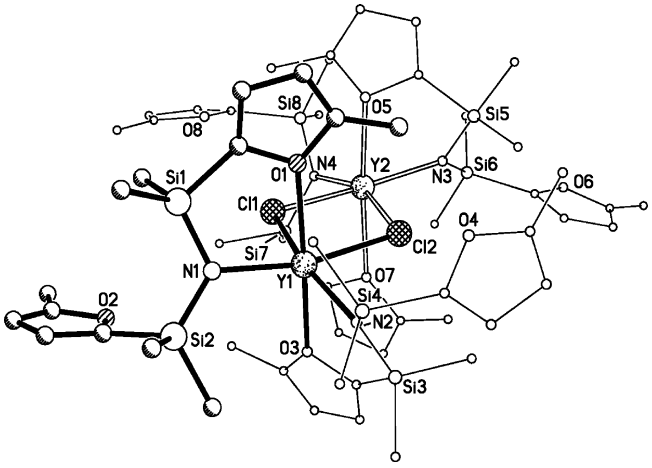

Fig. 10. Molecular structure of $[\mathbf{6}]_2$ with hydrogen atoms omitted and three of the four amide ligand reduced for clarity.

Table 8
Selected bond lengths (Å) and angles (°) for $[Y\{\mathbf{i}\}_2Cl]_2$ ($[\mathbf{6}]_2$).

Y1–N1	2.241(2)	Y2–N3	2.253(2)
Y1–N2	2.231(2)	Y2–N4	2.234(2)
Y1–O1	2.4106(17)	Y2–O5	2.475(2)
Y1–O3	2.3881(17)	Y2–O7	2.416(2)
Y1–Cl1	2.7511(7)	Y2–Cl1	2.7302(7)
Y1–Cl2	2.7693(7)	Y2–Cl2	2.7437(7)
N1–Y1–N2	105.08(8)	N3–Y2–N4	105.54(8)
N1–Y1–O1	82.80(7)	N3–Y2–O5	82.37(7)
N1–Y1–O3	98.59(7)	N3–Y2–O7	97.57(7)
N1–Y1–Cl1	92.25(6)	N3–Y2–Cl2	93.18(6)
N2–Y1–O1	108.40(7)	N4–Y2–O5	108.23(7)
N2–Y1–O3	80.81(7)	N4–Y2–O7	81.63(7)
N2–Y1–Cl2	90.86(6)	N4–Y2–Cl1	89.81(6)
O1–Y1–Cl1	83.28(4)	O5–Y2–Cl1	86.29(5)
O1–Y1–Cl2	90.02(5)	O5–Y2–Cl2	84.24(4)
O3–Y1–Cl1	86.85(5)	O7–Y2–Cl1	91.41(5)
O3–Y1–Cl2	86.09(5)	O7–Y2–Cl2	85.63(4)
Cl1–Y1–Cl2	72.530(19)	Cl1–Y2–Cl2	73.246(19)
Y1–Cl1–Y2	107.54(2)	Y1–Cl2–Y2	106.64(2)

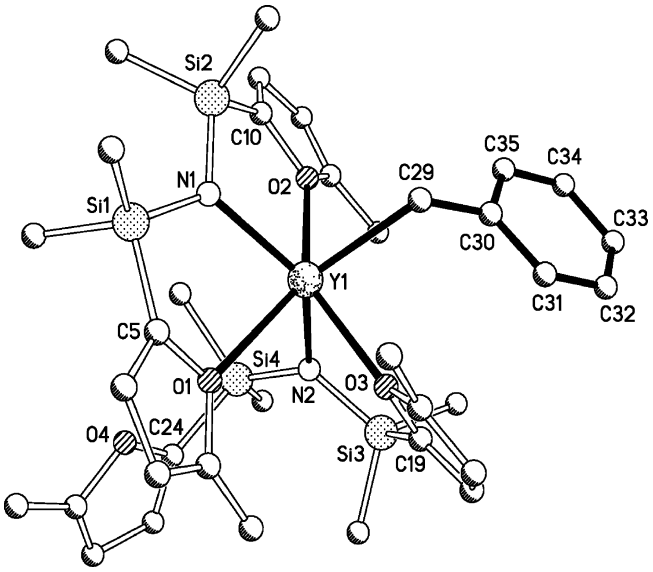

Fig. 11. Molecular structure of one of the independent molecules of **7**, with hydrogen atoms omitted.

Table 9
Selected bond lengths (Å) and angles (°) for $Y\{\mathbf{i}\}_2(CH_2Ph)$ (**7**) {molecule 2}.

Y1–N1	2.258(2) {2.259(2)}	Y1–N2	2.255(2) {2.264(2)}
Y1–C29	2.420(3) {2.422(2)}	Y1–O1	2.703(2) {2.691(2)}
Y1–O2	2.566(2) {2.561(2)}	Y1–O3	2.446(2) {2.444(2)}
N1–Si1	1.704(2) {1.707(2)}	N1–Si2	1.708(2) {1.708(2)}
N2–Si3	1.712(3) {1.711(2)}	N2–Si4	1.711(3) {1.715(3)}
N1–Y1–N2	132.13(9) {131.94(9)}	N1–Y1–C29	99.86(10) {99.22(10)}
N1–Y1–O1	76.79(7) {77.32(7)}	N1–Y1–O2	78.62(7) {78.46(7)}
N1–Y1–O3	134.18(8) {134.26(7)}	N2–Y1–C29	122.42(10) {123.12(10)}
N2–Y1–O1	90.49(7) {90.95(7)}	N2–Y1–O2	87.87(7) {88.37(7)}
N2–Y1–O3	79.42(7) {79.99(7)}	C29–Y1–O1	129.59(9) {128.38(9)}
C29–Y1–O2	78.91(9) {78.09(9)}	C29–Y1–O3	79.40(9) {79.17(9)}
O1–Y1–O2	145.04(6) {146.59(6)}	O1–Y1–O3	69.86(6) {69.36(6)}
O2–Y1–O3	143.43(6) {142.85(7)}	Y1–C29–C30	119.2(2) {120.3(2)}

3.4. Synthesis of the cationic yttrium complex, $[Y\{\mathbf{i}\}_2][B(C_6F_5)_3(CH_2Ph)]$ (**8**)

Many catalytic applications rely on the generation of a cationic metal centre at some point during the catalytic cycle [7]. A brief investigation was therefore carried out to assess whether amide {**i**} would be a suitable ancillary ligand in such systems. The yttrium benzyl **7** was chosen as a representative substrate, and was reacted with $B(C_6F_5)_3$ on an NMR scale. Generation of an ionic system was initially indicated by formation of an oil in C_6D_6. Subsequent removal of this solvent and addition of CD_2Cl_2 afforded a clear solution which was examined by ^1H NMR spectroscopy.

Strong evidence for the formation of ion pair $[Y\{\mathbf{i}\}_2][B(C_6F_5)_3(CH_2Ph)]$ (**8**) originates from loss of the coupling between CH_2Ph and ^{89}Y in the ^1H NMR spectrum, with the resultant signal broadened by interaction with the quadrupolar boron. A large downfield shift of δ 1.19 ppm accompanies these changes, although a change of NMR solvent was necessitated by insolubility of the ion pair in C_6D_6. One ligand environment was observed for the amide protons, although several different bonding scenarios are consistent with these data, as noted above. The salt was obtained as an analytically pure solid by precipitation from pentane.

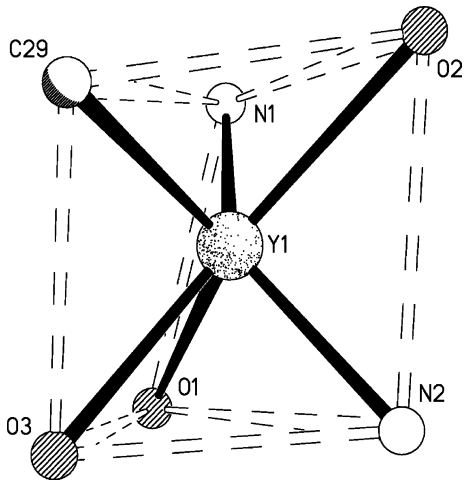

Fig. 12. Trigonal prismatic coordination geometry at the yttrium metal Y1 from compound **7**.

3.5. Preliminary survey of the catalytic potential of group 3 compounds

Two different areas of catalysis have been explored using the compounds described in this work; the scandium compound $Sc\{\mathbf{i}\}(CH_2SiMe_3)_2$ (**2**) was examined in the context of olefin polymerization and the yttrium compound $Y\{\mathbf{i}\}_2(CH_2Ph)$ (**7**) was investigated for intramolecular hydroamination catalysis.

3.5.1. Scandium mediated olefin polymerization

A preliminary assessment of compound **2** as a precatalyst in olefin polymerization catalysis was conducted (Table 10). The *in situ* conversion of the dialkyl scandium to a cationic metal was assumed to take place upon reaction with co-catalysts $[HNMe_2Ph][B(C_6F_5)_4]$, $[H(OEt_2)_2][B(3,5\text{-}\{CF_3\}_2C_6H_3)_4]$ or $[Ph_3C][B(C_6F_5)_4]$. A toluene solution containing this mixture was exposed to ethylene at ambient temperature and pressure for 1 h. Any solid polymer product was isolated and analyzed by high temperature GPC.

Table 10 shows the results for catalytic runs using **2** and each of the activators listed above. Given the quantities of precatalyst used, the activities can, at best, be described as 'poor', as outlined by the Gibson scale of activity [6,68]. The polymer itself was shown to be high molecular weight, with broad (multi-modal) molecular weight distributions, consistent with ill-defined catalysis. This is not too surprising given the presumed high reactivity of any cat-

Table 10
Catalytic activity of **2** for ethene polymerisation.

Run	Quantity of catalyst (mg {mmol})	Co-catalyst	Time (min)	Yield PE (g)	Activity (g mmol^{-1} h^{-1})	M_w ($\times 10^5$)	M_n ($\times 10^3$)	M_w/M_n
1	100 {0.20}	$[HNMe_2Ph][B(C_6F_5)_4]$	60	0.05	0.5	4.32	8.79	50
2	50 {0.10}	$[H(OEt_2)_2][B(3,5\text{-}\{CF_3\}_2C_6H_3)_4]$	60	0.04	0.4	2.28	5.44	42
3	100 {0.20}	$[Ph_3C][B(C_6F_5)_4]$	60	0.31	1.6			

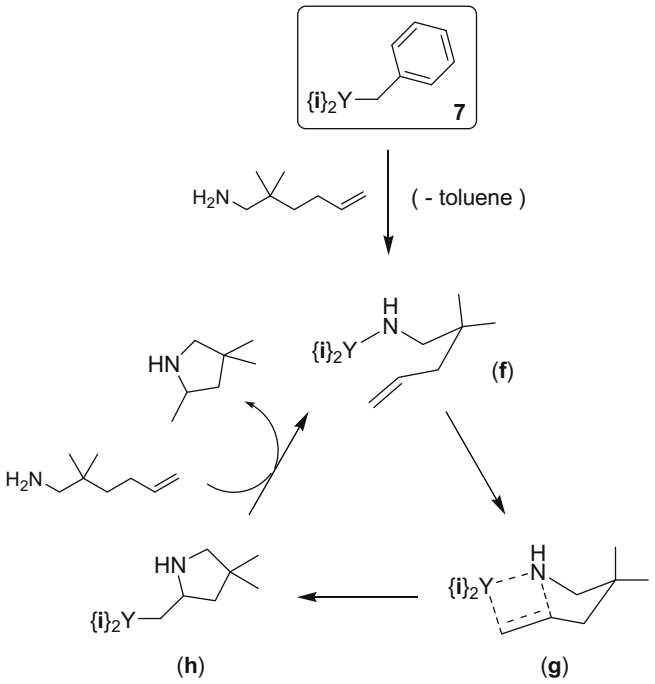

Scheme 3. Catalytic hydroamination with **7** as precatalyst and 2,2-dimethyl-1-aminopent-4-ene as substrate.

ionic metals generated, and likelihood of decomposition under catalytic testing conditions.

3.5.2. Yttrium mediated hydroamination

The yttrium benzyl compound $Y\{\mathbf{i}\}_2(CH_2Ph)$ (**7**) fits the traditional "L_2MR" formula (L = general ancillary ligand; R = alkyl group) for lanthanide compounds that have been shown to perform intramolecular hydroamination catalysis [69]. As such, the reaction between **7** and 2,2-dimethyl-1-aminopent-4-ene, the substrate typically used as a benchmark in these reactions, was carried out (Scheme 3).

NMR scale reactions performed in C_6D_6 have shown that the first step proceeds as expected, evidenced by disappearance of the ^{89}Y-coupled benzyl methylene resonance in the ^{1}H NMR spectrum, with the concomitant formation of toluene and the new yttrium species (**f**). This step is complete within 10 min. Cyclization was also observed to take place, affording the new alkyl derivative (**h**). However, the final protonolysis step liberating the product from the metal centre and regenerating (**f**) did not proceed spontaneously. Indeed, attempts to promote this step of the reaction by adding more substrate resulted in the formation of free ligand H-{**i**} in the reaction mixture, indicating that this system is not suitable for hydroamination catalysis under the conditions tested.

4. Conclusions

We have synthesized a series halide, alkyl and aryloxide compounds of the group 3 metals scandium and yttrium supported by the (furyl)-substituted disilazide ligand, $N\{SiMe_2R\}_2$ {**i**} (where R = 2-methylfuryl). Solution state NMR consistently indicated a single environment for the silyl groups of the amide ligands, consistent with static structures involving interaction of both or neither furyl groups with the metal, or the average signals of fluxional species. Single crystal X-ray diffraction show a number of different coordination modes and combinations thereof in the solid-state, suggesting solution-state fluxionality is the more accurate description of the NMR data. Formation of a cationic metal centre supported by {**i**} was demonstrated, by benzyl abstraction from the *bis*-amide yttrium compound, $Y\{\mathbf{i}\}_2(CH_2Ph)$. However, preliminary testing in selected catalytic conversions was disappointing, which is likely a combination of the highly reactive nature of these compounds, coupled with potential deactivation pathways involving reactivity with the ligands {**i**}.

Acknowledgement

We thank the University of Sussex for financial support.

Appendix A. Supplementary material

CCDC 740418, 740419, 740420, 740421, 740422, 740423 and 740424 contain the supplementary crystallographic data for $[\mathbf{1}]_2$, **2**, **3**, **4**, **5**, $[\mathbf{6}]_2$ and **7**. These data can be obtained free of charge from The Cambridge Crystallographic Data Centre via www.ccdc.cam.ac.uk/data_request/cif. Supplementary data associated with this article can be found, in the online version, at doi:10.1016/j.ica.2009.09.051.

References

[1] G.A. Molander, J.A.C. Romero, Chem. Rev. 102 (2002) 2161.
[2] Z. Hou, Y. Wakatsuki, Coord. Chem. Rev. 231 (2002) 1.
[3] J. Gromada, J.-F. Carpentier, A. Mortreux, Coord. Chem. Rev. 248 (2004) 397.
[4] Y. Nakayama, H. Yasuda, J. Organomet. Chem. 689 (2004) 4489.
[5] S. Arndt, J. Okuda, Adv. Synth. Catal. 347 (2005) 339.
[6] V.C. Gibson, S.K. Spitzmesser, Chem. Rev. 103 (2003) 283.
[7] P.M. Zeimentz, S. Arndt, B.R. Elvidge, J. Okuda, Chem. Rev. 106 (2006) 2404.
[8] S. Hong, T.J. Marks, Acc. Chem. Res. 37 (2004) 673.
[9] K.C. Hultzsch, Adv. Synth. Catal. 347 (2005) 367.
[10] M.F. Lappert, P.P. Power, A.V. Protchenko, A.L. Seeber, Metal Amide Chemistry, John Wiley & Sons, Ltd., Chippenham, 2009.
[11] L.T.J. Evans, F.G.N. Cloke, M.P. Coles, P.B. Hitchcock, Inorg. Chim. Acta 360 (2007) 1258.
[12] L.T.J. Evans, M.P. Coles, F.G.N. Cloke, P.B. Hitchcock, Dalton Trans. (2007) 2707.
[13] L.T.J. Evans, M.P. Coles, F.G.N. Cloke, P.B. Hitchcock, J. Organomet. Chem. 692 (2007) 2548.
[14] A.J. Rossini, R.W. Schurko, J. Am. Chem. Soc. 128 (2006) 10391.
[15] L. Lochmann, J. Trekoval, J. Organomet. Chem. 326 (1987) 1.
[16] F. Estler, G. Eickerling, E. Herdtweck, R. Anwander, Organometallics 22 (2003) 1212.
[17] K.C. Hultzsch, T.P. Spaniol, J. Okuda, Angew. Chem., Int. Ed. 38 (1999) 227.
[18] L.H. Sommer, W.P. Barie, J.R. Gould, J. Am. Chem. Soc. 75 (1953) 3765.
[19] P.B. Hitchcock, M.F. Lappert, A. Singh, J. Chem. Soc., Chem. Commun. (1983) 1499.
[20] G.M. Sheldrick, SHELXL-97, Program for the Refinement of Crystal Structures, Göttingen, 1997.
[21] R.C. Weast (Ed.), CRC Handbook of Chemistry and Physics, CRC Press, Florida, 1978.
[22] M. Karl, G. Seybert, W. Massa, K. Dehnicke, Z. Anorg. Allg. Chem. 625 (1999) 375.
[23] M.D. Fryzuk, G.R. Giesbrecht, S.J. Rettig, Organometallics 15 (1996) 3329.
[24] J.L. Atwood, K.D. Smith, J. Chem. Soc., Dalton Trans. (1973) 2487.
[25] J. Hitzbleck, J. Okuda, Organometallics 26 (2007) 3227.

[26] S. Arndt, P. Voth, T.P. Spaniol, J. Okuda, Organometallics 19 (2000) 4690.
[27] D.J.H. Emslie, W.E. Piers, M. Parvez, R. McDonald, Organometallics 21 (2002) 4226.
[28] A.W. Addison, T.N. Rao, J. Reedijk, J. van Rijn, G.C. Verschoor, J. Chem. Soc., Dalton Trans. (1984) 1349.
[29] Y. Luo, J. Baldamus, Z. Hou, J. Am. Chem. Soc. 126 (2004) 13910.
[30] X. Li, J. Baldamus, Z. Hou, Angew. Chem., Int. Ed. 44 (2005) 962.
[31] J. Blackwell, C. Lehr, Y. Sun, W.E. Piers, S.D. Pearce-Batchilder, M.J. Zaworotko, V.G. Young Jr., Can. J. Chem. 75 (1997) 702.
[32] A. Lara-Sanchez, A. Rodriguez, D.L. Hughes, M. Schormann, M. Bochmann, J. Organomet. Chem. 663 (2002) 63.
[33] S. Bambirra, M.W. Boukamp, A. Meetsma, B. Hessen, J. Am. Chem. Soc. 126 (2004) 9182.
[34] R.G. Howe, C.S. Tredget, S.C. Lawrence, S. Subongkoj, A.R. Cowley, P. Mountford, Chem. Commun. (2006) 223.
[35] B.R. Elvidge, S. Arndt, T.P. Spaniol, J. Okuda, Dalton Trans. (2006).
[36] Y. Yang, K. Liu, W. Gao, D. Cui, X. Chen, X. Jing, Organometallics 26 (2007) 4575.
[37] S. Ge, A. Meetsma, B. Hessen, Organometallics 26 (2007) 5278.
[38] S. Li, W. Miao, T. Tang, D. Cui, X. Chen, X. Jing, J. Organomet. Chem. 692 (2007) 4943.
[39] S. Li, W. Miao, T. Tang, W. Dong, X. Zhang, D. Cui, Organometallics 27 (2008) 718.
[40] M. Zimmermann, K.W. Törnroos, R.M. Waymouth, R. Anwander, Organometallics 27 (2008) 4310.
[41] M.E. Thompson, S.M. Baxter, A.R. Bulls, B.J. Burger, M.C. Nolan, B.D. Santarsiero, W.P. Schaefer, J.E. Bercaw, J. Am. Chem. Soc. 109 (1987) 203.
[42] M.E.G. Skinner, B.R. Tyrrell, B.D. Ward, P. Mountford, J. Organomet. Chem. 647 (2002) 145.
[43] C.S. Tredget, S.C. Lawrence, B.D. Ward, R.G. Howe, A.R. Cowley, P. Mountford, Organometallics 24 (2005) 3136.
[44] G.B. Deacon, P.E. Fanwick, A. Gitlits, I.P. Rothwell, B.W. Skelton, A.H. White, Eur. J. Inorg. Chem. (2001) 1505.
[45] S.C. Lawrence, B.D. Ward, S.R. Dubberley, C.M. Kozak, P. Mountford, Chem. Commun. (2003) 2880.
[46] Y. Luo, M. Nishiura, Z. Hou, J. Organomet. Chem. 692 (2007) 536.
[47] B. Liu, D. Cui, J. Ma, X. Chen, X. Jing, Chem. Eur. J. 13 (2007) 834.
[48] S. Bambirra, M.J.R. Brandsma, E.A.C. Brussee, A. Meetsma, B. Hessen, J.H. Teuben, Organometallics 19 (2000) 3197.
[49] A.A. Trifonov, D.M. Lyubov, G.K. Fukin, E.V. Baranov, Y.A. Kurskii, Organometallics 25 (2006) 3935.
[50] S. Bambirra, E. Otten, D. van Leusen, A. Meetsma, B. Hessen, Z. Anorg. Allg. Chem. 632 (2006) 1950.
[51] D.M. Lyubov, G.K. Fukin, A.A. Trifonov, Inorg. Chem. 46 (2007) 11450.
[52] S. Ge, A. Meetsma, B. Hessen, Organometallics 27 (2008) 3131.
[53] X. Liu, X. Shang, T. Tang, N. Hu, F. Pei, D. Cui, X. Chen, X. Jing, Organometallics 26 (2007) 2747.
[54] X. Xu, X. Xu, Y. Chen, J. Sun, Organometallics 27 (2008) 758.
[55] W.A. Herrmann, R. Anwander, F.C. Munck, W. Scherer, V. Dufaud, N.W. Huber, G.R.J. Artus, Z. Naturforsch., B: Chem. Sci. 49 (1994) 1789.
[56] W.A. Herrmann, F.C. Munck, G.R.J. Artus, O. Runte, R. Anwander, Organometallics 16 (1997) 682.
[57] M. Westerhausen, M. Hartmann, A. Pfitzner, W. Schwarz, Z. Anorg. Allg. Chem. 621 (1995) 837.
[58] C.J. Schaverien, A.G. Orpen, Inorg. Chem. 30 (1991) 4968.
[59] W.J. Evans, J.M. Olofson, J.W. Ziller, Inorg. Chem. 28 (1989) 4309.
[60] C.J. Schaverien, J.H.G. Frijns, H.J. Herres, J.R. van den Hende, J.H. Teuben, A.L. Spek, J. Chem. Soc., Chem. Commun. (1991) 642.
[61] G.B. Deacon, T. Feng, C.M. Forsyth, A. Gitlits, D.C.R. Hockless, Q. Shen, B.W. Skelton, A.H. White, J. Chem. Soc., Dalton Trans. (2000) 961.
[62] G.W. Gabe, M. Zhang-Presse, F.A. Riederer, G.P.A. Yap, Inorg. Chem. 42 (2003) 3527.
[63] P.B. Hitchcock, Q.-G. Huang, M.F. Lappert, X.-H. Wei, J. Mater. Chem. 14 (2004) 3266.
[64] A. Mandel, J. Magull, Z. Anorg. Allg. Chem. 622 (1996) 1913.
[65] A. Mandel, J. Magull, Z. Anorg. Allg. Chem. 623 (1997) 1542.
[66] S. Harder, C. Ruspic, N.N. Bhriain, F. Berkermann, M. Schürmann, Z. Naturforsch. B 63 (2008) 267.
[67] A.G. Avent, F.G.N. Cloke, B.R. Elvidge, P.B. Hitchcock, Dalton Trans. (2004) 1083.
[68] G.J.P. Britovsek, V.C. Gibson, D.F. Wass, Angew. Chem., Int. Ed. 38 (1999) 428.
[69] M.R. Gagné, T.J. Marks, J. Am. Chem. Soc. 111 (1989) 4108.